UCRL-52139

A REEVALUATION OF THE GAMMA-RAY ENERGIES AND ABSOLUTE BRANCHING INTENSITIES OF ^{237}U, $^{238,\ 239,\ 240,\ 241}Pu$, AND ^{241}Am

R. Gunnink, J. E. Evans, and A. L. Prindle

CIRCULATION COPY
SUBJECT TO RECALL
IN TWO WEEKS

October 11, 1976

Prepared for U.S. Energy Research & Development Administration under contract No. W-7405-Eng-48

LAWRENCE LIVERMORE LABORATORY
University of California/Livermore

Distribution Category
UC-34c

LAWRENCE LIVERMORE LABORATORY
University of California/Livermore, California/94550

UCRL-52139

A REEVALUATION OF THE GAMMA-RAY ENERGIES AND ABSOLUTE BRANCHING INTENSITIES OF ^{237}U, $^{238,\ 239,\ 240,\ 241}Pu$, AND ^{241}Am

R. Gunnink, J. E. Evans, and A. L. Prindle

MS. date: October 11, 1976

DISCLAIMER

This document was prepared as an account of work sponsored by an agency of the United States Government. Neither the United States Government nor the University of California nor any of their employees, makes any warranty, express or implied, or assumes any legal liability or responsibility for the accuracy, completeness, or usefulness of any information, apparatus, product, or process disclosed, or represents that its use would not infringe privately owned rights. Reference herein to any specific commercial product, process, or service by trade name, trademark, manufacturer, or otherwise, does not necessarily constitute or imply its endorsement, recommendation, or favoring by the United States Government or the University of California. The views and opinions of authors expressed herein do not necessarily state or reflect those of the United States Government or the University of California, and shall not be used for advertising or product endorsement purposes.

This report has been reproduced
directly from the best available copy.

Available to DOE and DOE contractors from the
Office of Scientific and Technical Information
P.O. Box 62, Oak Ridge, TN 37831
Prices available from (615) 576-8401, FTS 626-8401

Available to the public from the
National Technical Information Service
U.S. Department of Commerce
5285 Port Royal Rd.,
Springfield, VA 22161

Work performed under the auspices of the U.S. Department of Energy by Lawrence Livermore National Laboratory under Contract W-7405-ENG-48.

A REEVALUATION OF THE GAMMA-RAY ENERGIES AND ABSOLUTE BRANCHING INTENSITIES OF ^{237}U, $^{238,239,240,241}Pu$, AND ^{241}Am

Abstract

Promising new techniques for making quantitative measurements of plutonium require highly precise values of the gamma-ray energies and intensities for the isotopes involved. Using high isotopic purity sources and state of the art Ge(Li) detectors, we have reevaluated the energies and absolute emission probabilities of the gamma rays following the decay of ^{237}U, $^{238,239,240,241}Pu$, and ^{241}Am.

Introduction

Accurate analysis of a radioactive sample by Ge(Li) gamma-ray spectrometry requires correct information on the gamma-ray energies and intensities for each of the nuclides present in such a sample. Data for the isotopes of plutonium and for some of their daughter products have been previously reported.[1,2] However, new analytical techniques and methods have been developed, requiring better values. Consequently, we have measured many of the pertinent gamma-ray energy and intensity values associated with the decay of ^{237}U, $^{238,239,240,241}Pu$, and ^{241}Am.

The use of gamma-ray spectrometry to measure plutonium isotopic abundance ratios was one application in particular that prompted us to reevaluate the existing decay-scheme data.[3,4] In making such measurements, it is of course possible to use a direct calibration procedure, particularly for analyzing uniform and homogeneous samples.[5] Such a procedure would result in determining factors that convert peak intensities into grams or atoms of the specific isotopes represented by the peaks. Nonuniformly packaged or inhomogeneous samples are much more difficult to measure, however, because of uncertainties in counting efficiency and in gamma-ray attenuation by the sample matrix or other absorbing materials.

One way of minimizing the influences of these experimental

problems is to compute the isotopic ratios by using the peak intensities observed in a set of neighboring peaks that are produced by the various isotopes in the sample. Since the energies are nearly equal, the efficiency and attenuation differences will be quite small, and the ratio of isotopic abundances is then, to a first approximation, directly related to the peak intensities as follows:

$$A/B = \frac{I_1 \cdot t_A}{\varepsilon_1 \cdot Y_1} \; \frac{I_2 \cdot t_B}{\varepsilon_2 \cdot Y_2}$$

$$= \frac{I_1}{I_2} \cdot \frac{\varepsilon_2}{\varepsilon_1} \cdot \frac{Y_2}{Y_1} \cdot \frac{t_A}{t_B} ,$$

where

A/B = isotopic ratio

I_1 and I_2 = observed peak intensities of the two gamma rays coming from isotope A and B, respectively

ε_1 and ε_2 = gamma-ray counting efficiencies

Y_1 and Y_2 = the gamma yield or branching intensities of the respective gamma rays

t_A and t_B = the respective half-lives of isotopes A and B.

Although it may not be possible to obtain accurate absolute values for ε and Y individually, it is possible to get accurate ratios over a small energy range. The accuracy of the calculated isotopic ratio is then largely limited by the precision with which the peak intensities are measured.

A search for peak groupings that can potentially provide information on isotopic ratios indicates that nine such spectral regions do exist. Some of these regions are quite complex while others are simply doublets. The number of isotopic components and the accuracy with which ratio measurements can be made vary.

A computer program was written to simulate various sample counting conditions and the peak groupings were studied to indicate the type and quality of information that could possibly be obtained under various measurement conditions. The results of this study[3] indicate that many of the groupings are useful for determining isotopic ratios and therefore warranted the accurate measurement of the appropriate branching intensity ratios.

Summary of Experimental Procedures

Sources of high isotopic purity were prepared and measured using a variety of Ge detectors. The low-energy region was investigated using small sources to minimize absorption problems and using detectors with approximately 525 eV (FWHM) resolution at 122 keV. The higher energy regions required larger sources and larger detectors. These detectors ranged upward to 60 cm^3 in volume and had resolutions of less than 2 keV (FWHM) at 1.33 MeV.

A determination of the absolute branching intensity requires two quantities: (1) the number of photons of a given energy emitted by the sample, and 2) the total number of decays that occurred in the same time interval. The first requires a well-calibrated detector, methods of unfolding and interpreting peak intensities, a model for describing the detector efficiency and geometry, and methods for correcting for attenuations occurring within the sample or in external absorbers. The methods used to calculate gamma emission rates have been discussed in other reports.[6] In summary, we believe the detectors have a calibration accuracy of ± 2% and that the computational models are also capable of this accuracy. Algorithms have been found that very precisely fit the observed peak shapes,[6] and computer techniques were used for unfolding the complex peak multiplets (up to 12 peaks in a grouping).

The decay rate, which is the second necessary quantity, was obtained in different ways. Since most of the isotopes under consideration, except for ^{237}U and ^{241}Pu, are alpha-particle emitters, samples were prepared and assayed by standard alpha-counting techniques. The most prevalent alpha counter is the 2π counter, which has a counting efficiency of 51.7% when the sample is mounted on platinum. Other counting systems used were a low-geometry alpha counter (where the efficiency is determined by the simple restraints of geometry which can be calculated) and by 4π α-γ coincidence counting. The latter technique directly measures the disintegration rate of ^{241}Am samples since it has a rather abundant 59•keV gamma-ray emission in coincidence with the alpha-particle emissions. The 4π counting corrections were less than 1%, and a counting precision and reproducibility of 0.2% could be achieved.

Similar techniques were used to calibrate the ^{238}Pu, ^{239}Pu, and ^{240}Pu,

so that the assay errors for these solutions were well within 1%. We also confirmed the ^{239}Pu and ^{240}Pu assays by chemical analyses, using the controlled-potential coulometric-titration technique.

The ^{241}Pu solution was standardized by isotope-dilution mass spectrometry using the standardized ^{239}Pu as a tracer.

Using these calibration methods, we believe that the errors in the assays are certainly less than those attending the overall detector efficiency. However, as was discussed earlier, it was also important in the present study to measure the ratio of certain branching intensities (see above equation).

It is not difficult to get accurate gamma intensity ratios if the energies are nearly the same and the gamma emissions originate in the same isotope. The accuracy of such ratio measurements is limited largely by the statistical accuracy with which the two peak intensities can be measured. Our interest, however, is to measure such ratios for samples whose gamma emissions originate from different isotopes. These measurements also require a knowledge of the ratio of the disintegration rates of the respective isotopes involved.

The measurement of accurate intensity ratios requires (1) preparing mixed sources of appropriate strengths for good peak ratio measurements, (2) determining the atom ratio of the isotopes using mass spectrometry or alpha pulse-height analysis, and (3) calculating the decay rate ratio using the half-lives of the respective isotopes. Using this procedure, it was possible to obtain intensity ratio measurements that in most instances were within ± 1%.

Results

Table 1 summarizes some important intensity ratios we have measured directly and the error associated with the ratio. Using this data, and data from several other measurements, we have summarized the intensity relationships for nine important gamma-ray energy groupings (see Table 2).

The complete gamma-ray listings are quite similar to those published earlier, although there are several additions and a few deletions. However, errors associated with the new values, particularly in the nine critical regions shown in Table 2, have been reduced significantly. The errors associated with the

Table 1. Measured branching intensity ratios for some important plutonium isotope gamma rays.

Isotopes (γ-energies)	γ-intensity branching ratio (error)
^{238}Pu (43)/^{240}Pu (45)	0.865 (0.6)
^{238}Pu (99)/^{240}Pu (104)	1.037 (0.6)
^{241}Pu (148)/^{239}Pu (144)	0.660 (1.0)
^{241}Pu (148)/^{239}Pu (146)	1.57 (1.0)
^{238}Pu (152)/^{240}Pu (160)	2.379 (1.0)
^{240}Pu (160)/^{239}Pu (161)	3.33 (1.0)
^{241}Pu-U(164)/^{239}Pu (161)	0.378 (1.0)
^{241}Pu (208)/^{239}Pu (203)	0.950 (0.5)
^{240}Pu (642)/^{239}Pu (646)	0.840 (1.0)

intensity values in Tables 3-9 reflect, principally, the statistical uncertainty in the measurement of peak areas.

^{238}Pu ($t_{1/2}$ = 87.7 yr)

High isotopic purity sources of ^{238}Pu are available so that there is very little contamination from the other plutonium isotopes. However, many (α,xn) reactions can occur producing a number of gamma-emitting contaminants. It is somewhat difficult to determine which gamma rays belong to ^{238}Pu without additional experimentation. Fortunately, the prominent gamma rays belonging to ^{238}Pu are well established, and the others are not important for analytical considerations. For these reasons, we have not changed the gamma-ray listing significantly other than to revise the energy and intensity values shown in Table 3. The germanium spectra are shown in Figs. 1 and 2.

^{239}Pu ($t_{1/2}$ = 24 150 yr)

Several different sources were counted ranging from a few milligrams to 15 gms and from 99.1% to 99.999% isotopic purity. Again the list of gamma rays is similar to that published

Table 2. Nine peak groupings useful for isotopic ratio determinations. Tabulations specify sources, energies, and intensities.

	Energy, keV	Intensity
	Group I	
^{238}Pu	43.477	3.92×10^{-4}
^{241}Pu	44.20	4.38×10^{-8}
^{241}Pu	44.86	8.36×10^{-9}
^{240}Pu	45.232	4.53×10^{-4}
^{239}Pu	46.21	6.83×10^{-6}
^{239}Pu	46.69	5.40×10^{-7}
^{239}Pu	51.629	2.70×10^{-4}
	Group II	
U x ray	94.660	(a)
^{239}Pu	96.150	2.23×10^{-7}
Np x ray	97.071	(b)
U x ray	98.441	(a)
^{239}Pu	98.780	1.22×10^{-5}
^{241}Am	98.951	2.03×10^{-4}
Pu x ray	99.530	(c)
^{238}Pu	99.864	7.24×10^{-5}
Np x ray	101.066	(b)
^{241}Am	102.966	1.95×10^{-4}
^{239}Pu	103.020	2.17×10^{-6}
^{241}Pu	103.680	1.01×10^{-6}
Pu x ray	103.748	(c)
^{240}Pu	104.244	6.98×10^{-5}

	Energy, keV	Intensity
	Group III	
110- to 121-keV region is very complex, including x rays and gamma rays from all the isotopes.		
^{241}Am	122.994	1.00×10^{-5}
^{239}Pu	123.62	1.97×10^{-7}
^{239}Pu	124.51	6.13×10^{-7}
^{239}Pu	125.21	7.11×10^{-7}
^{241}Am	125.292	4.08×10^{-5}
^{239}Pu	129.294	6.26×10^{-5}
	Group IV	
^{239}Pu	141.657	3.20×10^{-7}
^{239}Pu	143.350	1.73×10^{-7}
^{239}Pu	144.211	2.83×10^{-6}
^{239}Pu	146.077	1.19×10^{-6}
^{241}Am	146.557	4.61×10^{-6}
^{241}Pu	148.567	1.87×10^{-6}
^{241}Am	150.11	7.40×10^{-7}
^{238}Pu	152.68	9.56×10^{-6}
	Group V	
^{239}Pu	158.10	1.00×10^{-8}
^{241}Pu	159.955	6.74×10^{-8}

Table 2. (Continued)

	Energy, keV	Intensity
	Group V (Continued)	
^{239}Pu	160.19	6.20×10^{-8}
^{240}Pu	160.28	4.02×10^{-6}
^{239}Pu	161.45	1.20×10^{-6}
^{241}Pu-^{237}U	164.58	4.53×10^{-7}
^{241}Am	164.58	6.67×10^{-7}
^{241}Am	165.93	2.32×10^{-7}
	Group VI	
^{239}Pu	203.537	5.60×10^{-6}
^{241}Pu-^{237}U	208.000	5.33×10^{-6}
^{241}Am	208.000	7.91×10^{-6}
	Group VII	
^{241}Pu-^{237}U	332.354	2.98×10^{-7}
^{241}Am	332.354	1.49×10^{-6}
^{239}Pu	332.838	5.06×10^{-6}
^{241}Pu-^{237}U	335.405	2.39×10^{-8}
^{241}Am	335.405	4.96×10^{-6}
^{239}Pu	336.107	1.134×10^{-6}
^{239}Pu	341.510	6.62×10^{-7}
^{239}Pu	345.014	5.59×10^{-6}
	Group VIII	
^{239}Pu	367.050	8.65×10^{-7}
^{239}Pu	368.550	9.03×10^{-7}
^{241}Pu-^{237}U	368.605	1.05×10^{-8}
^{241}Am	368.605	2.17×10^{-6}
^{241}Pu-^{237}U	370.934	2.71×10^{-8}
^{241}Am	370.934	5.23×10^{-7}
^{239}Pu	375.042	1.57×10^{-5}
^{241}Am	376.595	1.38×10^{-6}
^{239}Pu	380.166	3.05×10^{-6}
^{239}Pu	382.751	2.59×10^{-6}
	Group IX	
^{241}Am	633.0	1.26×10^{-8}
^{239}Pu	633.15	2.53×10^{-8}
^{239}Pu	637.837	2.56×10^{-8}
^{239}Pu	640.075	8.20×10^{-8}
^{241}Am	641.42	7.10×10^{-8}
^{240}Pu	642.48	1.245×10^{-7}
^{239}Pu	645.969	1.49×10^{-7}
^{239}Pu	649.321	7.12×10^{-9}
^{239}Pu	650.529	2.70×10^{-9}

Table 2. (Continued)

	Energy, keV	Intensity		Energy, keV	Intensity
	Group IX (Continued)			Group IX (Continued)	
^{239}Pu	652.074	6.55×10^{-8}	^{239}Pu	658.929	9.69×10^{-8}
^{241}Am	652.96	3.77×10^{-7}	^{241}Am	662.420	3.64×10^{-6}
^{239}Pu	654.880	2.25×10^{-8}	^{239}Pu	644.587	1.657×10^{-8}

[a] Uranium L/K x rays result from the decay of all of the plutonium isotopes. Refer to subsequent tables for intensity data.

[b] Neptunium L/K x rays result from the decay of ^{237}U and ^{241}Am. Refer to subsequent tables for intensity data.

[c] These plutonium x rays may be present in a spectrum due to the alpha- and gamma-induced x-ray fluorescence process.

earlier. However, the energies and branching intensities have been improved, particularly in the critical regions discussed earlier. The assignment of some of the low-intensity, high-energy gamma rays to ^{239}Pu may be somewhat tenuous, since they may have been produced by (α,xn) reactions. Table 4 lists our current best values. Figs. 3 and 4 show typical germanium spectra of ^{239}Pu.

^{240}Pu ($t_{1/2}$ = 6 537 yr)

Although high isotopic purity sources of ^{240}Pu were used, small amounts of ^{241}Pu are generally present. However, this does not present a problem in measuring the prominent gamma rays of ^{240}Pu. Since it is an even-even nuclide like ^{238}Pu and ^{242}Pu, its low-energy spectra are very similar, as Figs. 1 and 5 show, being dominated by the gamma cascade of the 0+, 2+, 4+, 6+ ground-state rotational band. As with ^{238}Pu, the high-energy region shown in Fig. 6 is complicated by (α,xn) reactions and from activities coming from the spontaneous fissioning of ^{240}Pu. Table 5 lists the data for the low-energy and the two most intense high-energy gamma rays.

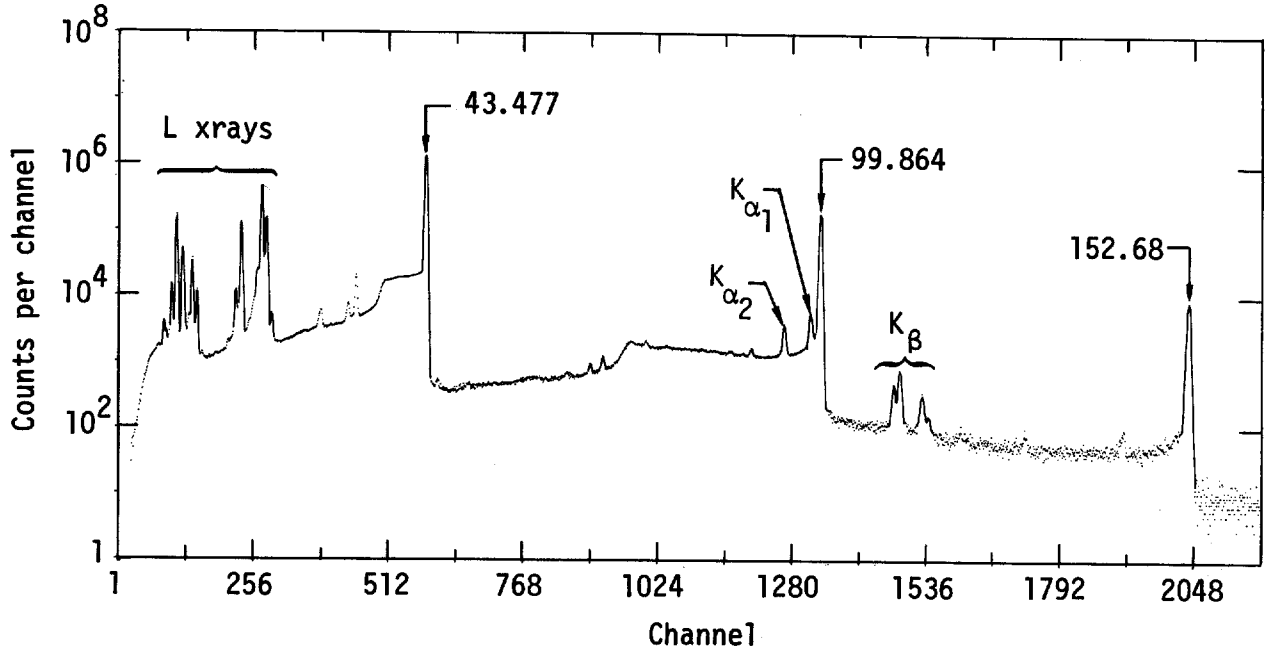

Fig. 1. Low-energy spectrum of ^{238}Pu.

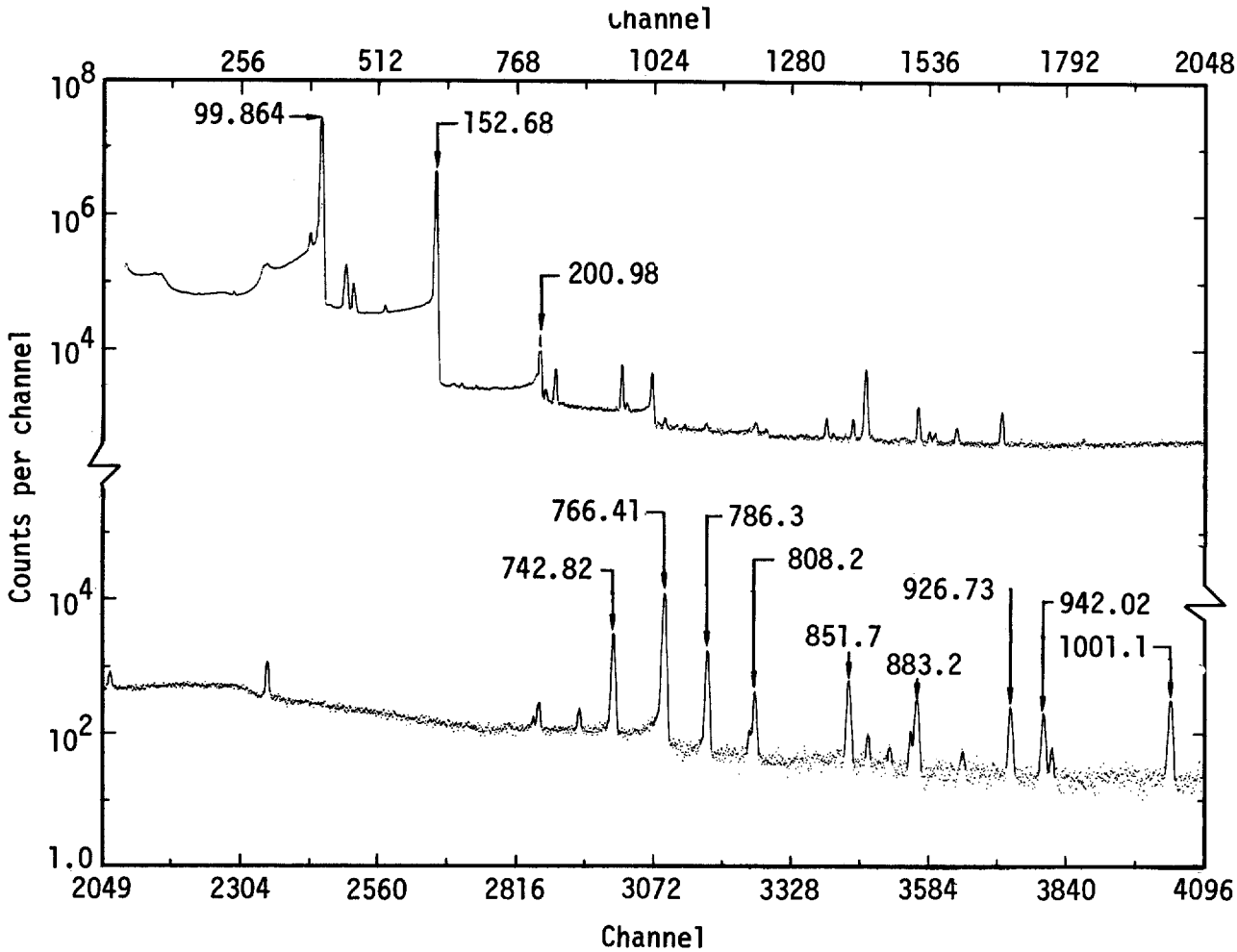

Fig. 2. High-energy spectrum of ^{238}Pu. Many of the peaks may be due to (α, xn)-type reactions occurring in the sample.

^{241}Pu - ^{237}U ($t_{1/2}$ = 14.5 yr)

The decay of ^{241}Pu is principally by β^- emission to ^{241}Am. However, a small amount of α-decay to ^{237}U ($t_{1/2}$ = 6.75 d) does occur, resulting in the presence of gamma rays from its decay. The ^{237}U spectra, shown in Fig. 7, has many of the same gamma rays that ^{241}Am has because both decay to levels of ^{237}Np. These direct interferences must be properly recognized in interpreting spectra containing these two isotopes.

The intensity of the α-branch has been remeasured to be 0.00246% ± 0.00001%, which agrees with our earlier value.[2] The accurate alpha measurement of ^{241}Pu also allowed us to get an accurate measurement of the ^{237}U gamma-ray intensities. These are given in Table 6.

Samples of ^{241}Pu were chemically purified from the ^{237}U and ^{241}Am daughter products. Although spectra were taken immediately following purification, ^{237}U grows in quickly, as Fig. 8 shows. Gamma-ray energy and intensities are shown in Table 7.

^{241}Am ($t_{1/2}$ = 433 yr)

Many spectra were taken of the various energy regions, using sources ranging from small massless sources to 100-mg sources. Since the very low-energy region (10 to 30 keV) is frequently used for calibrating detectors in this region, particular attention was given to unfolding the complex set of L x-rays that contribute to this region. Fig. 9 shows its complexity. Although it is difficult to completely unfold all of the structure present, Table 8 is a list of the components we observed. The data presented here agree well with those summarized recently by Campbell and McNelles.[7]

As Fig. 10 shows, ^{241}Am also has many higher energy gamma rays. These are listed in Table 9.

Any analysis of the 94- to 104-keV region requires an analysis of the K_α x-rays corresponding to uranium, neptunium, and plutonium. The x-rays, however, exhibit a different line shape from gamma rays of equivalent energy.[8] The data tabulated in Table 10 are useful for determining the x-ray relative peak positions, intensities, and intrinsic line widths.

Table 3. Gamma rays of ^{238}Pu.

	Energy	Intensity, γ/dis	Error	Energy	Intensity, γ/dis	Error
	43.477±0.005	3.93×10^{-4}	(0.3)	705.6	5.03×10^{-10}	(40)
$K_{\alpha 2}$	94.658±0.005	1.05×10^{-6}	(1.4)	708.4	5.00×10^{-9}	(10)
$K_{\alpha 1}$	98.442±0.005	1.69×10^{-6}	(1.0)	742.82	5.17×10^{-8}	(1)
	99.864±0.005	7.24×10^{-5}	(0.2)	766.41	2.19×10^{-7}	(0.6)
$K_{\beta 3}$	110.421	2.00×10^{-7}		786.3	3.28×10^{-8}	(1.0)
K_{β_1}	111.300	3.90×10^{-7}		805.4	1.29×10^{-9}	(15)
K_{β_4}	114.333			808.2	8.00×10^{-9}	(3)
K_{β_2}	114.561	1.58×10^{-7}		851.7	1.29×10^{-8}	(2)
K_{β_x}	115.40					
	152.68±0.02	9.56×10^{-6}	(0.5)			
	200.98	4.08×10^{-8}	(2)			

Table 4. Gamma rays of ^{239}Pu.

	Energy	Intensity, γ/dis	Error	Energy	Intensity, γ/dis	Error
	30.04	2.17×10^{-6}	(3)	123.62	1.97×10^{-7}	(6)
	38.664	1.05×10^{-4}	(1.0)	124.51	6.13×10^{-7}	(3)
	40.41	1.62×10^{-6}	(10)	125.21	7.11×10^{-7}	(2)
	42.06	1.65×10^{-6}	(3)	129.294±0.010	6.26×10^{-5}	(0.2)
	46.21	7.37×10^{-6}	(10)	141.657	3.20×10^{-7}	(2)
	46.69	5.80×10^{-7}	(6)	143.350	1.73×10^{-7}	(4)
	51.629±0.010	2.70×10^{-4}	(0.2)	144.211	2.83×10^{-6}	(0.6)
	54.040	2.00×10^{-6}	(1.4)	146.077	1.190×10^{-5}	(0.6)
	56.838	1.13×10^{-5}	(1.0)	158.1	1.00×10^{-8}	(10)
	65.741	4.53×10^{-7}	(4)	160.19	6.20×10^{-8}	(20)
	67.67	1.61×10^{-6}	(2)	161.450±0.015	1.20×10^{-6}	(0.4)
	68.72	5.10×10^{-6}	(1)	167.81	2.93×10^{-8}	(25)
	77.607	3.90×10^{-6}	(0.7)	171.344	1.105×10^{-6}	(0.8)
	78.42	1.52×10^{-6}	(1.4)	173.70	3.05×10^{-8}	(25)
	(89.59)			179.19	6.58×10^{-7}	(1)
U K_{α_2}	94.660±0.005	4.22×10^{-5}	(0.25)	184.55	2.12×10^{-8}	(30)
	96.13	2.23×10^{-7}	(20)	188.23	1.09×10^{-7}	(10)
U K_{α_1}	98.441±0.005	6.76×10^{-5}	(0.3)	189.32	8.30×10^{-7}	(2)
	98.780	1.22×10^{-5}	(3)	193.	8.87×10^{-8}	(10)
	103.020±0.020	2.17×10^{-6}	(1.6)	195.66	1.064×10^{-6}	(0.5)
	110.421	7.95×10^{-6}	(0.8)	196.87	3.70×10^{-8}	(12)
	111.300	1.55×10^{-5}	(0.6)	203.537	5.60×10^{-6}	(0.2)
	111.89	3.07×10^{-7}	(10)	225.37	1.56×10^{-7}	(4)
K_{β_2}	114.333	6.28×10^{-6}	(2)	(227.)		
K_{β_4}	114.561			237.38	1.44×10^{-7}	(4)
K_{β_x}	115.38	6.49×10^{-6}	(1.5)	242.08	7.31×10^{-8}	(7)
	116.26	5.97×10^{-6}	(1.5)	243.38	2.53×10^{-7}	(2)
	119.708	3.00×10^{-7}	(2)	244.92	5.10×10^{-8}	(10)
				248.95	7.24×10^{-8}	(10)
				255.38	8.05×10^{-7}	(2)
				263.93	2.61×10^{-7}	(3)

Table 4. (Continued)

Energy	Intensity, γ/dis	Error	Energy	Intensity γ/dis	Error
265.7	1.58×10^{-8}	(25)	428.4	1.00×10^{-8}	(10)
281.2	2.15×10^{-8}	(15)	430.08	4.30×10^{-8}	(3)
285.3	1.91×10^{-8}	(20)	445.72	8.70×10^{-8}	(2)
297.49	5.02×10^{-7}	(2)	446.82	8.45×10^{-9}	(15)
302.87	5.13×10^{-8}	(8)	451.474	1.89×10^{-6}	(0.3)
307.85	5.47×10^{-8}	(7)	457.61	1.49×10^{-8}	(1)
311.74	2.58×10^{-7}	(2)	461.25	2.27×10^{-8}	(1)
316.41	1.36×10^{-7}	(3)	463.9	2.78×10^{-9}	(10)
319.68	4.80×10^{-8}	(10)	473.9	5.36×10^{-10}	(50)
320.88	5.36×10^{-7}	(1)	481.54	4.60×10^{-8}	(0.6)
323.81	5.42×10^{-7}	(1)	487.06	2.65×10^{-9}	(8.0)
332.838	5.060×10^{-6}	(0.2)	493.08	8.68×10^{-9}	(3.0)
336.107	1.134×10^{-6}	(0.3)	497.0	4.61×10^{-10}	(50)
341.510	6.62×10^{-7}	(0.4)	526.4	5.72×10^{-10}	(30)
345.014	5.592×10^{-6}	(0.2)	538.8	3.05×10^{-9}	(6)
350.8	1.75×10^{-8}	(20)	550.5	4.22×10^{-9}	(6)
354.0	7.31×10^{-9}	(40)	557.3	3.82×10^{-10}	(50)
361.89	1.22×10^{-7}	(5)	579.4	8.58×10^{-10}	(20)
367.050	8.65×10^{-7}	(0.3)	582.89	6.15×10^{-9}	(3)
368.550	9.03×10^{-7}	(0.3)	586.3	1.53×10^{-9}	(10)
375.042	1.570×10^{-5}	(0.1)	596.0	3.90×10^{-10}	(50)
380.166	3.051×10^{-6}	(0.2)	597.99	1.67×10^{-8}	(3)
382.751	2.587×10^{-6}	(0.2)	599.6	1.99×10^{-9}	(12)
392.53 }	5.527×10^{-6}	(0.2)	606.9	1.20×10^{-9}	(10)
393.14 }			608.9	1.16×10^{-9}	(10)
399.51	6.10×10^{-8}	(4)	612.83	9.46×10^{-9}	(5)
406.9	6.35×10^{-9}	(40)	617.10	1.34×10^{-8}	(5)
411.15	6.8×10^{-8}	(50)	618.28	2.04×10^{-8}	(3)
413.712	1.489×10^{-5}	(0.1)	619.21	1.21×10^{-8}	(6)
422.586	1.193×10^{-6}	(0.4)	624.78	4.57×10^{-9}	(4)
426.68	2.328×10^{-7}	(1.5)	633.15	2.53×10^{-8}	(1.2)

Table 4. (Continued)

Energy	Intensity, γ/dis	Error	Energy	Intensity, γ/dis	Error
637.837	2.56×10^{-8}	(1.2)	769.37	1.12×10^{-7}	(0.3)
640.075	8.20×10^{-8}	(0.6)	777.1	2.78×10^{-10}	(25)
645.969	1.489×10^{-7}	(0.4)	779.61	1.36×10^{-9}	(6)
649.321	7.12×10^{-9}	(7)	786.9	8.61×10^{-10}	(10)
650.529	2.70×10^{-9}	(15)	788.5	3.52×10^{-10}	(20)
652.074	6.55×10^{-8}	(0.6)	792.9	2.00×10^{-10}	(20)
654.880	2.25×10^{-8}	(1.2)	796.9	1.49×10^{-10}	(20)
658.929	9.69×10^{-8}	(0.7)	803.2	6.37×10^{-10}	(7)
664.587	1.657×10^{-8}	(1.6)	805.9	2.76×10^{-10}	(15)
668.2	3.93×10^{-10}	(30)	808.4	1.21×10^{-9}	(5)
670.8	8.60×10^{-11}	(50)	813.7	4.51×10^{-10}	(10)
674.05	5.15×10^{-9}	(3)	816.0	2.41×10^{-10}	(15)
685.97	8.73×10^{-9}	(3)	821.3	5.52×10^{-10}	(10)
688.1	1.11×10^{-9}	(10)	826.8	1.80×10^{-10}	(30)
690.81	5.57×10^{-9}	(5)	828.9	1.33×10^{-9}	(6)
693.2	5.00×10^{-10}	(30)	832.5	2.96×10^{-10}	(12)
697.8	7.35×10^{-10}	(20)	837.3	1.91×10^{-10}	(20)
699.6	7.91×10^{-10}	(20)	840.4	4.81×10^{-10}	(10)
701.1	5.12×10^{-9}	(3)	844.0	1.34×10^{-9}	(5)
703.73	3.95×10^{-8}	(0.4)	879.2	3.61×10^{-10}	(10)
712.96	5.16×10^{-10}	(12)	891.0	7.93×10^{-10}	(10)
714.71	7.85×10^{-10}	(10)	895.4	7.49×10^{-11}	(30)
717.72	2.74×10^{-8}	(0.4)	898.1	1.75×10^{-10}	(20)
720.3	4.85×10^{-10}	(10)	905.5	7.51×10^{-11}	(30)
727.9	1.24×10^{-9}	(5)	911.7	1.37×10^{-10}	(25)
736.5	3.00×10^{-10}	(30)	918.7	8.44×10^{-11}	(35)
742.7	3.75×10^{-10}	(30)	931.9	1.27×10^{-10}	(35)
747.4	8.07×10^{-10}	(20)	940.3	4.96×10^{-10}	(10)
756.40	3.47×10^{-8}	(0.4)	955.6	3.09×10^{-10}	(10)
763.7	3.24×10^{-10}	(50)	957.6	3.20×10^{-10}	(10)
766.6	2.75×10^{-9}	(5)	979.7	2.76×10^{-10}	(15)

Table 4. (Continued)

Energy	Intensity, γ/dis	Error	Energy	Intensity, γ/dis	Error
982.7	1.08×10^{-10}	(25)	1005.7	1.78×10^{-10}	(15)
986.9	2.09×10^{-10}	(20)	1009.4	1.40×10^{-10}	(20)
992.7	2.66×10^{-10}	(15)			

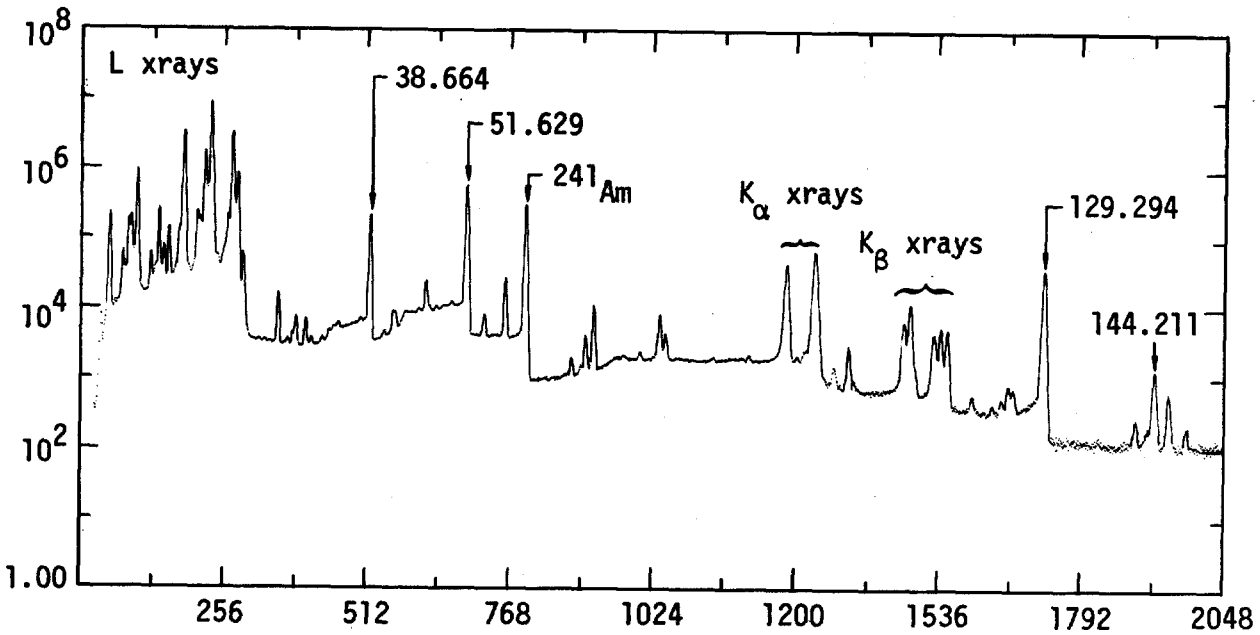

Fig. 3. Low-energy spectrum of ^{239}Pu.

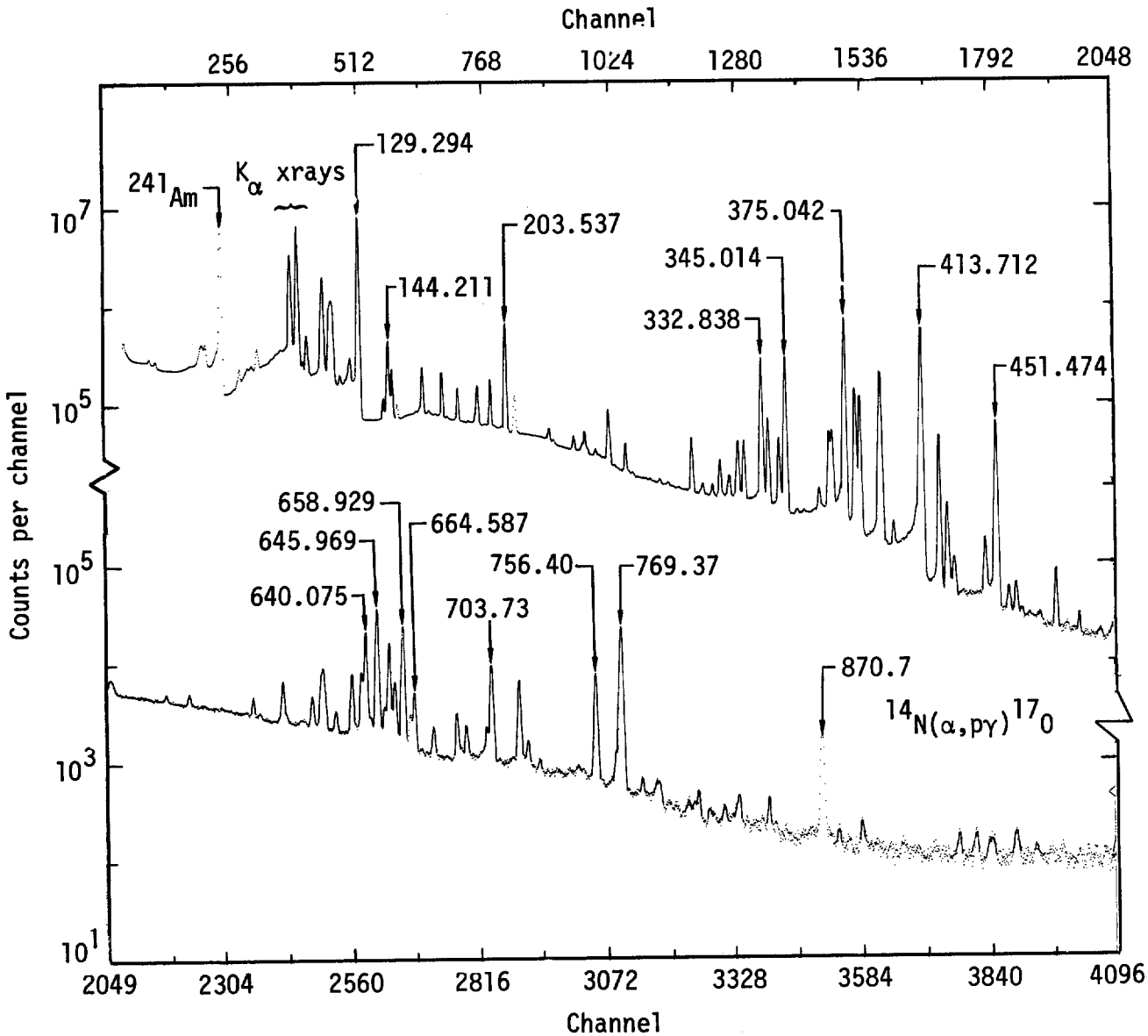

Fig. 4. Intermediate (upper) and high-energy (lower) spectra of ^{239}Pu.

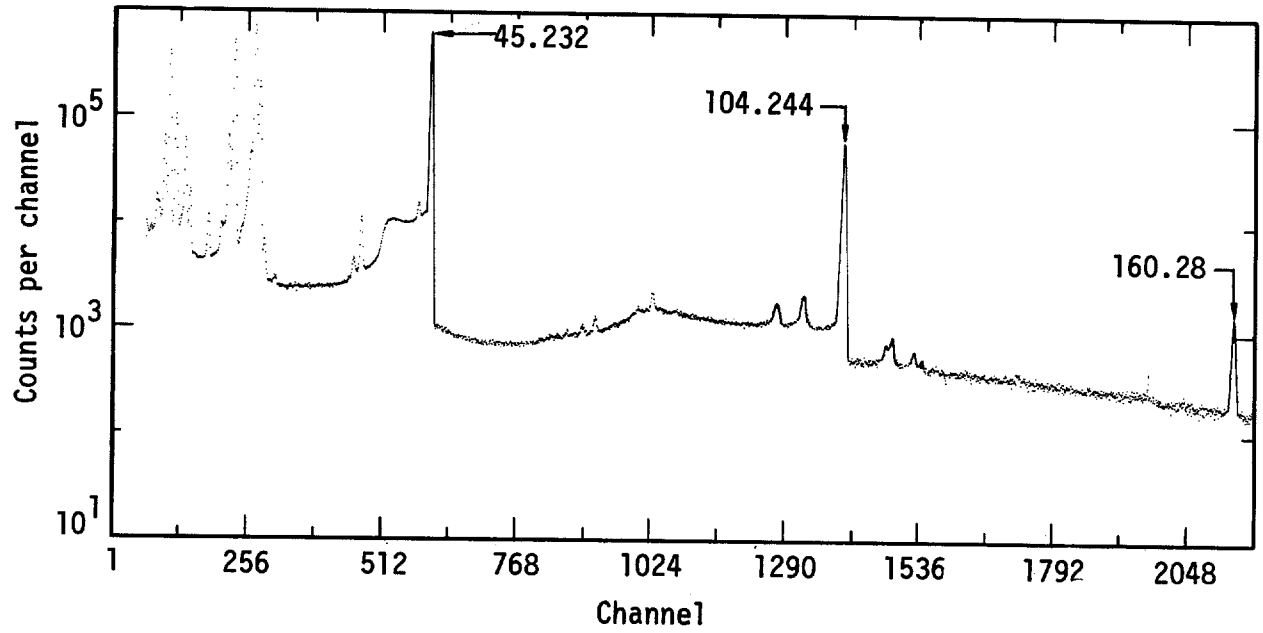

Fig. 5. Low-energy spectrum of ^{240}Pu.

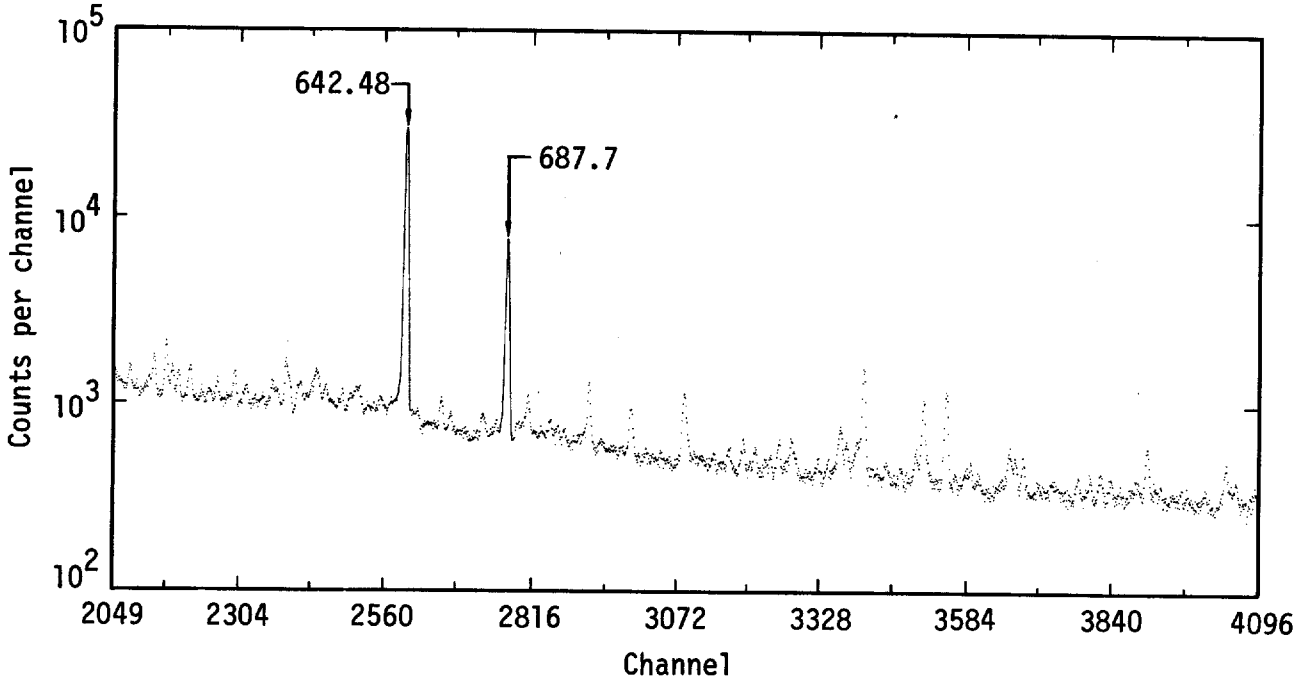

Fig. 6. High-energy spectrum of ^{240}Pu.

Table 5. Gamma rays of ^{240}Pu.

	Energy	Intensity, γ/dis	Error		Energy	Intensity, γ/dis	Error
	45.232±0.005	4.53×10^{-4}	(0.2)	K_{β_4}	114.333		
K_{α_2}	94.658±0.005	6.36×10^{-7}	(5)	K_{β_2}	114.561	9.32×10^{-8}	
K_{α_1}	98.422±0.005	1.02×10^{-6}	(5)	K_{β_x}	115.40		
	104.244±0.005	6.98×10^{-5}	(0.4)		160.280±0.015	4.02×10^{-6}	(0.7)
K_{β_3}	110.421	1.18×10^{-7}			642.48	1.245×10^{-7}	(1)
K_{β_1}	111.300	2.30×10^{-7}			687.7	3.55×10^{-8}	(1.5)

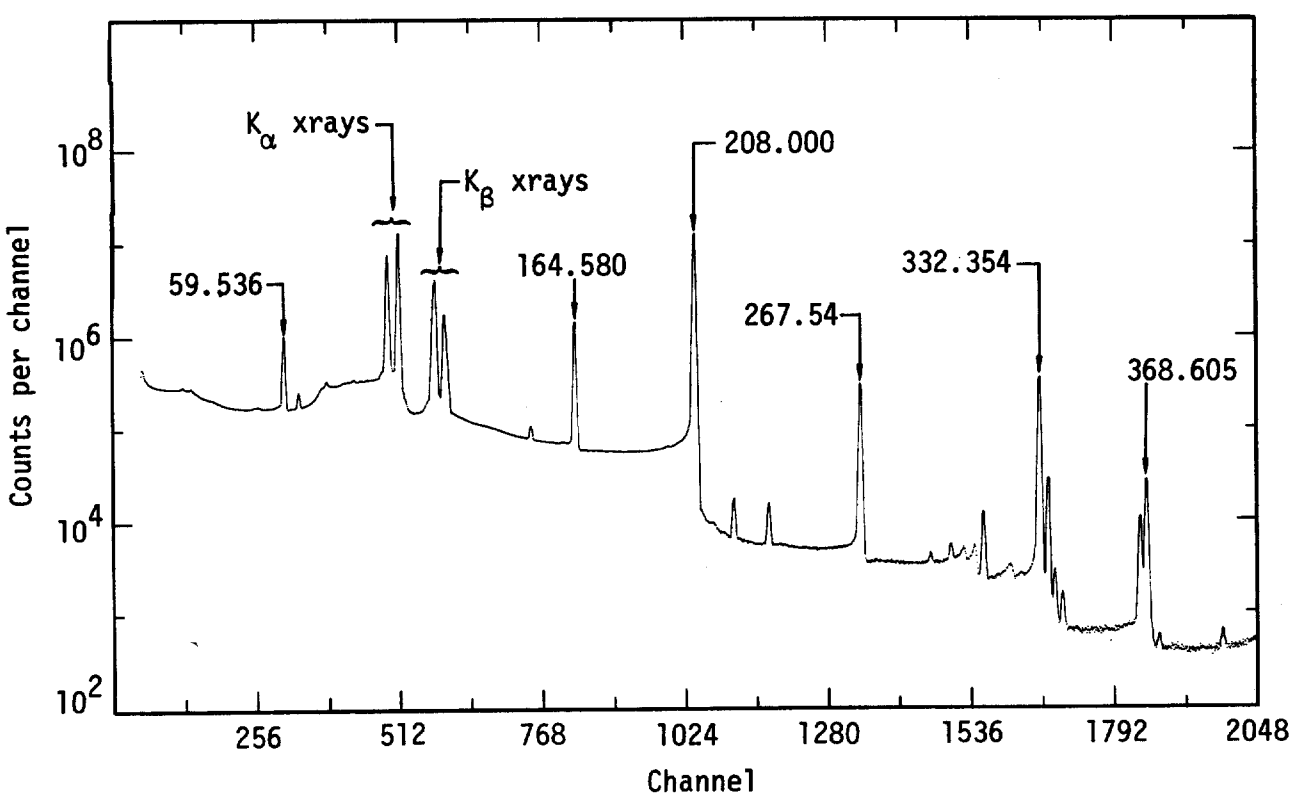

Fig. 7. Spectrum of ^{237}U.

Table 6. Gamma rays of ^{237}U.[a]

	Energy	Intensity, γ/dis	Error	Energy	Intensity, γ/dis	Error
	26.34	2.43×10^{-2}	(0.5)	164.580	1.84×10^{-2}	(0.5)
	33.19	1.30×10^{-3}	(1.6)	208.000±0.010	2.17×10^{-1}	(0.2)
	43.43	2.40×10^{-4}	(7)	221.73	2.12×10^{-4}	(2)
	51.005	3.40×10^{-3}	(2)	234.24	2.05×10^{-4}	(2)
	59.536±0.003	3.45×10^{-1}	(0.2)	267.54	7.40×10^{-3}	(0.5)
	64.832	1.30×10^{-2}	(0.5)	332.354	1.21×10^{-2}	(0.3)
K_{α_2}	97.071±0.005	1.58×10^{-1}	(0.4)	335.405	9.70×10^{-4}	(1.0)
K_{α_1}	101.066±0.005	2.52×10^{-1}	(0.3)	337.75	8.90×10^{-5}	(5)
K_{β_3}	113.300	3.04×10^{-2}	(0.5)	340.45	1.65×10^{-5}	(20)
K_{β_1}	114.230	5.85×10^{-2}	(0.3)	368.605	4.29×10^{-4}	(2)
K_{β_5}	114.950	3.35×10^{-3}	(10)	370.934	1.103×10^{-3}	(1.4)
K_{β_4}	117.340	7.90×10^{-3}				
K_{β_2}	117.580	1.56×10^{-2}				
K_{β_x}	118.43	8.23×10^{-3}				

[a] ^{241}Pu α-branching probability to ^{237}U has been measured to be 0.00246% ± 0.00001%.

Table 7. Gamma rays of ^{241}Pu.

	Energy	Intensity, γ/dis	Error		Energy	Intensity, γ/dis	Error
	44.20	4.18×10^{-8}		K_{β_1}	111.300	1.09×10^{-6}	(1)
	44.86	8.36×10^{-9}					
	56.32	2.50×10^{-8}		K_{β_5}	111.89	3.31×10^{-8}	
	56.76	9.75×10^{-9}					
	71.6	2.86×10^{-8}	(10)	K_{β_2}	114.34	1.60×10^{-7}	
	77.10	2.22×10^{-7}	(3)	K_{β_4}	114.56	3.64×10^{-7}	
K_{α_2}	94.658±0.005	3.03×10^{-6}	(0.5)				
				K_{β_x}	115.40	1.34×10^{-7}	
K_{α_1}	98.442±0.005	4.85×10^{-6}	(0.5)				
					121.2	6.85×10^{-9}	
	103.680±0.005	1.01×10^{-6}	(0.6)		148.567±0.010	1.87×10^{-6}	(0.3)
K_{β_3}	110.421	5.90×10^{-7}	(1.5)		159.955	6.74×10^{-8}	

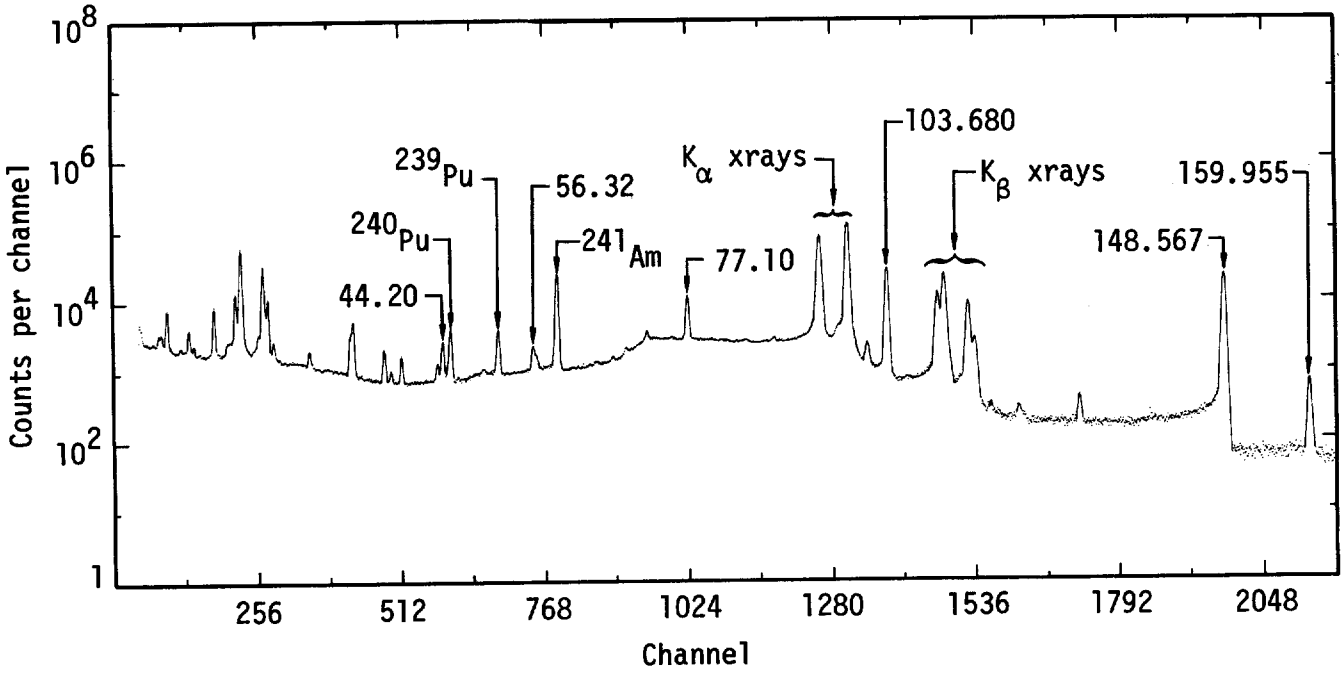

Fig. 8. Spectrum of ^{241}Pu.

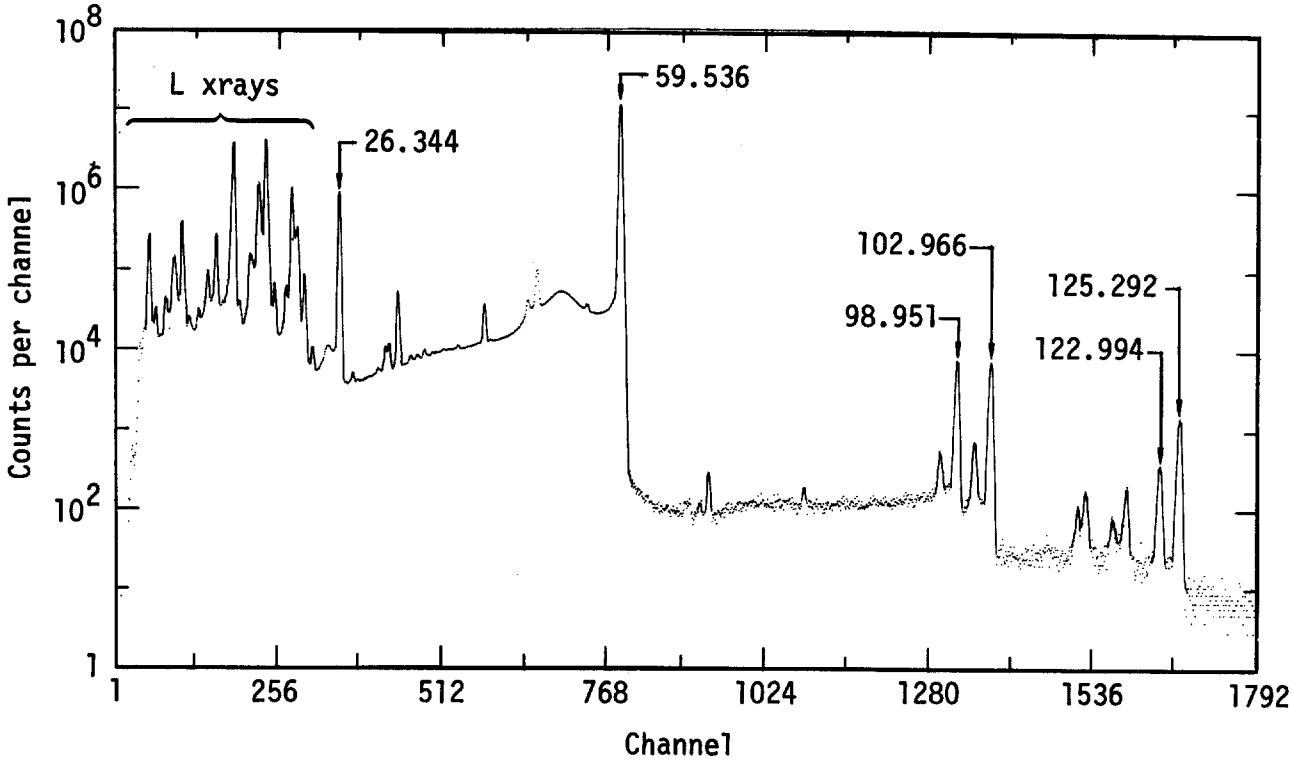

Fig. 9. Low-energy spectrum of ^{241}Am.

Table 8. L x-ray region of ^{241}Am.

Energies		Intensity, photons/dis		
11.87	L_ℓ	8.06×10^{-3}		
13.37		1.9×10^{-3}		
13.72	L_{α_2}	1.45×10^{-2}	0.132	
13.95	L_{α_1}	1.15×10^{-1}		
15.9		9.0×10^{-3}		
16.4				
16.93	L_{β_2}	5.00×10^{-2}		0.201
17.75	L_{β_4}, L_{β_5}, L_{β_1}	1.40×10^{-1}	0.192	
18.67	$L_{\beta_{9-10}}$	2.00×10^{-3}		
20.10	L_{γ_5}	1.58×10^{-3}		
20.80	$L_{\gamma_1}+L_{\gamma_2}$	3.25×10^{-2}		
21.41	L_{γ_3}	1.26×10^{-2}	0.0494	
22.21	L_{γ_4}	2.75×10^{-3}		
23.13		1.85×10^{-4}		

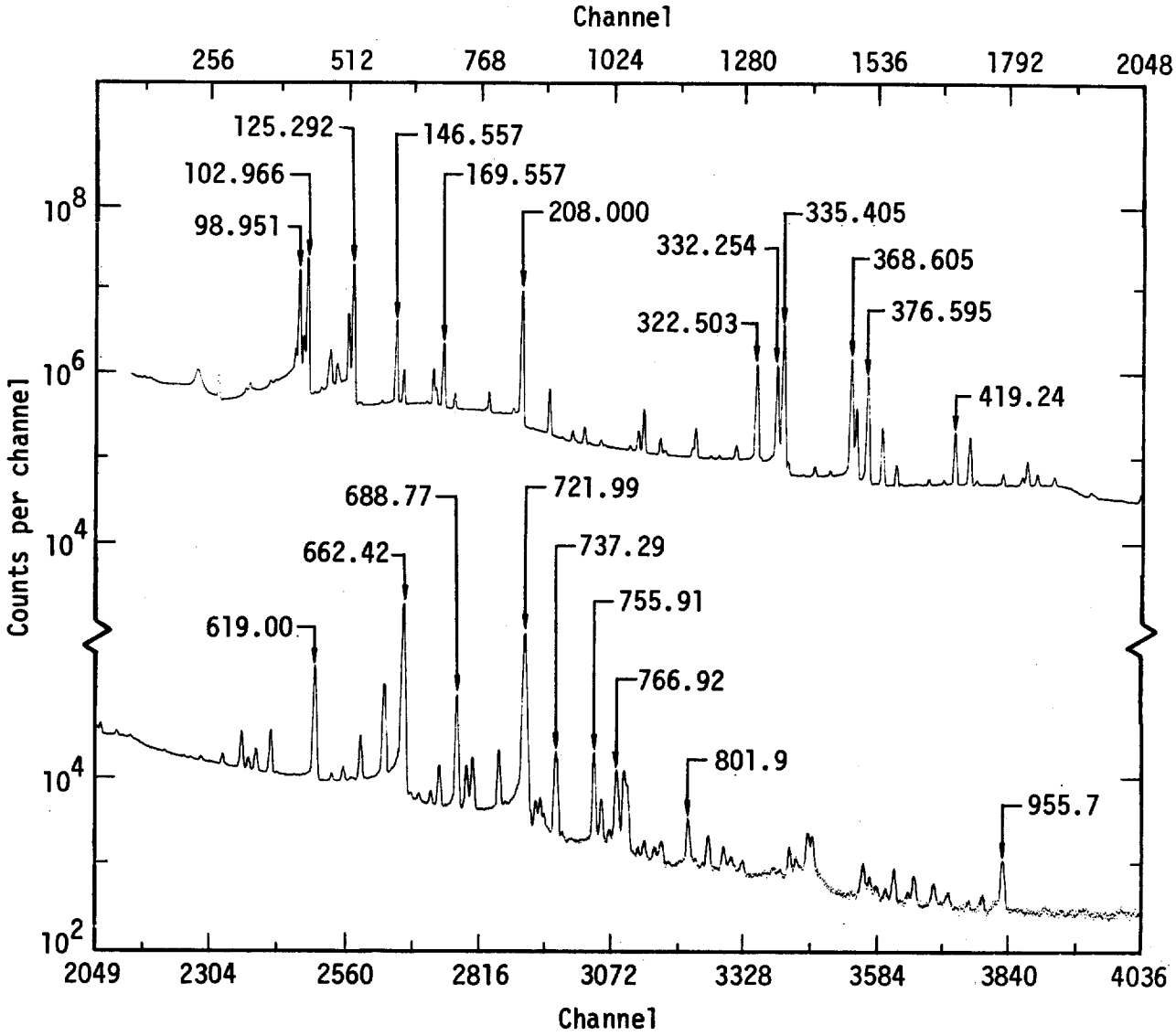

Fig. 10. High-energy spectrum of ^{241}Am.

Table 9. Gamma rays of ^{241}Am.

	Energy	Intensity, γ/dis	Error	Energy	Intensity, γ/dis	Error
	26.344	2.45×10^{-2}	(0.1)	203.87	2.90×10^{-8}	(6)
	32.183	1.74×10^{-4}	(1)	208.000	7.91×10^{-6}	(0.5)
	33.197	1.26×10^{-3}	(0.3)	221.73	4.24×10^{-7}	(1)
	59.536±0.003	.359		233.87	4.64×10^{-8}	(6)
K_{α_2}	97.072±0.005	1.18×10^{-5}	(2)	234.33	6.57×10^{-9}	(40)
				246.70	2.42×10^{-8}	(10)
	98.951±0.005	2.03×10^{-4}	(0.5)	260.90	1.21×10^{-8}	(15)
K_{α_1}	101.066±0.005	1.90×10^{-5}	(1.4)	264.85	9.04×10^{-8}	(4)
	102.966±0.005	1.95×10^{-4}	(0.5)	267.54	2.63×10^{-7}	(2)
K_{α_3}	113.300	2.37×10^{-6}		271.58	6.37×10^{-9}	(30)
				275.68	6.57×10^{-8}	(5)
K_{β_1}	114.230	4.72×10^{-6}		291.21	3.08×10^{-8}	(10)
				292.78	1.42×10^{-7}	(3)
K_{β_5}	114.950			304.23	1.01×10^{-8}	(20)
K_{β_4}	117.340			322.503	1.518×10^{-6}	(0.6)
		2.30×10^{-6}		332.354	1.490×10^{-6}	(0.3)
K_{β_2}	117.580			335.405	4.960×10^{-6}	(0.3)
				337.72	4.29×10^{-8}	(5)
K_{β_x}	118.43			350.56	1.19×10^{-8}	(20)
	122.994±0.010	1.00×10^{-5}	(0.8)	358.36	1.20×10^{-8}	(20)
	125.292±0.010	4.08×10^{-5}	(0.5)	368.605	2.17×10^{-6}	(0.3)
	139.53	5.34×10^{-8}	(20)	370.934	5.23×10^{-7}	(0.8)
	146.557±0.010	4.61×10^{-6}	(1)	376.595	1.383×10^{-6}	(0.7)
	150.11	7.40×10^{-7}	(2)	383.74	2.82×10^{-7}	(1.5)
	(159.06)	1.4×10^{-8}	(30)	390.54	5.90×10^{-8}	(4)
	164.580	6.67×10^{-7}	(3)	406.37	1.45×10^{-8}	(15)
	165.93	2.32×10^{-7}	(4)	419.24	2.87×10^{-7}	(2)
	169.557	1.73×10^{-6}	(1)	426.39	2.46×10^{-7}	(2)
	175.09	1.82×10^{-7}	(5)	429.84	1.15×10^{-8}	(20)
	190.40	2.19×10^{-8}	(20)	442.75	3.52×10^{-8}	(7)
	191.90	2.16×10^{-7}	(4)	452.21	2.40×10^{-8}	(10)

Table 9. (Continued)

Energy	Intensity, γ/dis	Error	Energy	Intensity, γ/dis	Error
454.62	9.70×10^{-8}	(3)	737.29	8.00×10^{-8}	(3)
459.59	3.63×10^{-8}	(7)	755.91	7.60×10^{-8}	(3)
467.98	2.88×10^{-8}	(7)	759.46	1.67×10^{-8}	(5)
486.3	1.00×10^{-8}	(30)	763.4	1.96×10^{-9}	(30)
(512.0)	1.15×10^{-8}	(20)	766.92	5.00×10^{-8}	(3)
514.2	2.58×10^{-8}	(10)	770.58	4.74×10^{-8}	(4)
522.0	9.46×10^{-9}	(30)	772.13	2.66×10^{-8}	(5)
574.0	1.25×10^{-8}	(15)	777.2	6.10×10^{-10}	(50)
(582.6)	2.32×10^{-9}	(50)	780.5	2.50×10^{-9}	(20)
586.52	1.31×10^{-8}	(15)	788.8	3.88×10^{-9}	(15)
590.28	2.86×10^{-8}	(7)	801.9	1.36×10^{-8}	(10)
597.42	7.41×10^{-8}	(4)	811.8	6.05×10^{-9}	(12)
619.00	5.94×10^{-7}	(1)	819.3	4.00×10^{-9}	(15)
627.2	5.64×10^{-9}	(30)	822.6	2.18×10^{-9}	(25)
633.0	1.26×10^{-8}	(15)	828.5	2.43×10^{-9}	(25)
641.42	7.10×10^{-8}	(4)	851.5	3.77×10^{-9}	(15)
652.96	3.77×10^{-7}	(2)	854.7	2.00×10^{-9}	(20)
662.420	3.64×10^{-6}	(0.3)	859.2	8.16×10^{-10}	(30)
669.9	3.80×10^{-9}	(30)	862.6	5.34×10^{-9}	(10)
675.8	6.40×10^{-9}	(20)	887.5	2.22×10^{-9}	(20)
680.06	3.13×10^{-8}	(5)	898.4	7.22×10^{-10}	(40)
688.77	3.25×10^{-7}	(1.5)	902.5	3.00×10^{-9}	(15)
693.49	3.68×10^{-8}	(4)	912.4	2.50×10^{-9}	(20)
696.44	5.34×10^{-8}	(3)	922.2	1.91×10^{-9}	(20)
709.41	6.41×10^{-8}	(2)	928.8	5.52×10^{-10}	(50)
721.990	1.96×10^{-6}	(0.4)	945.7	5.60×10^{-10}	(50)
729.52	1.33×10^{-8}	(10)	955.7	5.78×10^{-9}	(10)
731.5	4.70×10^{-9}	(30)			

Table 10. K_α x-ray energies, intensities, and intrinsic line widths for uranium, neptunium, and plutonium.

Source	Energy, keV[a]	Intensity ratio	Line width, eV	Source	Energy, keV[a]	Intensity ratio	Line width, eV
U K_{α_1}	94.660	0.625	104	Np K_{α_2}	101.066		
U K_{α_2}	98.441			Pu K_{α_1}	99.530	0.630	112
Np K_{α_1}	97.071	0.628	108	Pu K_{α_2}	103.748		

[a]Errors associated with the x-ray energies are ± 2eV relative to one another.

References

1. J.E. Cline, *Gamma Rays Emitted by the Fissionable Nuclides and Associated Isotopes*, Idaho Nuclear Corp., Idaho Falls, Idaho, Rept. IN-1448 (1920) and ANCR-1069 (1972).
2. R. Gunnink and R.J. Morrow, *Gamma-Ray Energies and Absolute Branching Intensities for* $^{238,239,240,241}Pu$ *and* ^{241}Am, Lawrence Livermore Laboratory, Rept. UCRL-51087 (1971).
3. R. Gunnink, *A Simulation Study of Plutonium Gamma Ray Groupings for Isotopic Ratio Determinations*, Lawrence Livermore Laboratory, Rept. UCRL-51605 (1974).
4. J. Parker and T.D. Reilly, Los Alamos Progress Rept. LA-5675-PR, Aug. 1974.
5. R. Gunnink, J.B. Niday, and P.D. Siemens, *A System for Plutonium Analysis by Gamma Ray Spectrometry*, Lawrence Livermore Laboratory, Rept. UCRL-51577 (1974).
6. R. Gunnink and J.B. Niday, *Computerized Quantitative Analysis by Gamma-Ray Spectrometry*, Lawrence Livermore Laboratory, Rept. UCRL-51061 (1971).
7. J.L. Campbell and L.A. McNelles, *Nucl. Instrum. Methods 125*, 205 (1975).
8. R. Gunnink, *An Algorithm for Fitting Lorentzian-broadened K-series X-ray Peaks of the Heavy Elements*, Lawrence Livermore Laboratory, Rept. UCRL-78707 (to be published in *Nucl. Instrum. Methods*).

BHK/gw /po/wl/gw